JAERI-M
86-056

RADIATION LOSS AND GLOBAL ENERGY BALANCE OF OHMICALLY HEATED DIVERTOR DISCHARGE IN JT-60 TOKAMAK

March 1986

Yoshihiko KOIDE, Kimio YAMADA,* Hidetoshi YOSHIDA
Hiroo NAKAMURA, Setsuo NIIKURA** and Shunji TSUJI

日本原子力研究所
Japan Atomic Energy Research Institute

JAERI-Mレポートは，日本原子力研究所が不定期に公刊している研究報告書です。
入手の問合わせは，日本原子力研究所技術情報部情報資料課（〒319-11茨城県那珂郡東海村）あて，お申しこしください。なお，このほかに財団法人原子力弘済会資料センター（〒319-11 茨城県那珂郡東海村日本原子力研究所内）で複写による実費頒布をおこなっております。

JAERI-M reports are issued irregularly.
Inquiries about availability of the reports should be addressed to Information Division Department of Technical Information, Japan Atomic Energy Research Institute, Tokai-mura, Naka-gun, Ibaraki-ken 319-11, Japan.

編集兼発行　日本原子力研究所
印　　刷　㈱高野高速印刷

RADIATION LOSS AND GLOBAL ENERGY BALANCE OF OHMICALLY HEATED DIVERTOR DISCHARGE IN JT-60 TOKAMAK

Yoshihiko KOIDE, Kimio YAMADA*, Hidetoshi YOSHIDA
Hiroo NAKAMURA, Setsuo NIIKURA** and Shunji TSUJI

Department of Large Tokamak Research
Naka Fusion Research Establishment
Japan Atomic Energy Research Institute
Naka-machi, Naka-gun, Ibaraki-ken

(Received February 21, 1986)

Divertor experiment in JT-60 with a small divertor chamber has been successfully performed up to 1.6 MA discharge. Several divertor effects were experimentally confirmed as follows.

Radiation loss in main plasma saturates with the increase of plasma current and its ratio to the input power is about 20 % at 1.5 MA. The rest of input power is exhausted into the divertor chamber and a half of it is dissipated as the radiation loss.

Impurity accumulation is not observed during a few sec without internal MHD activity and gross impurity confinement time is several hundred msec.

Keywords: Tokamak, JT-60, Divertor, Radiation Loss, Global Energy Balance, Remote Cooling.

---

* On leave from Energy Research Laboratory, Hitachi, Ltd.

** On leave from Mitsubishi Atomic Power Industries, Inc.

ＪＴ－60のオーミック加熱時のダイバーター放電における放射損失とエネルギーバランス

日本原子力研究所那珂研究所臨界プラズマ研究部
小出芳彦・山田喜美雄*・吉田英俊
中村博雄・新倉節夫**・辻　俊二

（１９８６年２月２１日受理）

小型のダイバーター室を有するＪＴ－60装置において，1.6ＭＡの安定なダイバーター放電を達成し，以下のダイバーター効果を確認した。

メインプラズマからの放射損失はプラズマ電流の増加に対して飽和の傾向を示し，入力パワーに対する割合は，1.5ＭＡ時で２０％程度となった。その他の入力パワーは，ダイバーター室へ導かれ，その内の約５０％が放射損失となっている。内部ＭＨＤ振動のない数秒間のフラットトップの間，不純物のプラズマ中心への集中は観測されず，その閉じ込め時間は数１００ msec であった。

那珂研究所：茨城県那珂郡那珂町大字向山
* 外来研究員　；　日立エネルギー研究所
** 外来研究員　；　三菱原子力工業（株）

Contents

目　　次

1. INTRODUCTION

Problems of impurity control and plasma-wall interactions have become more serious in recent high power heating tokamak experiments. Divertor is a promising way to solve these problems, which was demonstrated in small and medium sized devices such as DIVA [1], Doublet-III [2] and ASDEX [3]. In these experiments, following favorable results have been obtained;

1) Radiation loss in main plasma was reduced.
2) Major fraction of total heating power was diverted from the main chamber to the divertor chamber.
3) Significant fraction of it was dissipated by radiation and heat load to divertor plates was alleviated in high density discharges.

In addition to these divertor functions, recent high power heating experiments indicate that good confinement discharges (so called H-mode) are obtained almost only at the tokamaks with divertor [4,5].

It is very important to demonstrate these favorable ability in a reactor grade tokamak and to extraporate a poloidal divertor to a reactor. In a reactor, only a shallow open divertor with a small burial chamber could be applied. JT-60 is a large tokamak with a simple poloidal divertor like that. The initial experiment was carried out from April to June in 1985 and stable 1.6 MA divertor discharge was obtained [6].

In this paper, radiation loss and global energy balance are discussed. Experiments are performed with ohmically heated hydrogen discharges: plasma current I_p of (0.5 ~ 1.6) MA, toroidal field B_T of (3 ~ 4) T, line-average electron density $\bar{n}_e$ of (0.5 ~ 4) $\times 10^{19}$ m^{-3}. Major and minor radii are 3.15 m and 0.83 m, respectively.

In the following section, experimental arrangements are described. Requirement for divertor effects are treated in section 3. Section 4 deals with the characteristics of radiation loss. Global energy balance is discussed in section 5. Impurity behavior is treated in section 6. In section 7, summary and conclusion are presented.

2. EXPERIMENTAL ARRANGEMENTS

Figure 1 shows the poloidal cross section of JT-60. It has a poloidal divertor on the outer equatorial plane. The first wall consists of toroidal limiters (Mo), liners (Inconel 625) and divertor

1. INTRODUCTION

Problems of impurity control and plasma-wall interactions have become more serious in recent high power heating tokamak experiments. Divertor is a promising way to solve these problems, which was demonstrated in small and medium sized devices such as DIVA [1], Doublet-III [2] and ASDEX [3]. In these experiments, following favorable results have been obtained;

1) Radiation loss in main plasma was reduced.
2) Major fraction of total heating power was diverted from the main chamber to the divertor chamber.
3) Significant fraction of it was dissipated by radiation and heat load to divertor plates was alleviated in high density discharges.

In addition to these divertor functions, recent high power heating experiments indicate that good confinement discharges (so called H-mode) are obtained almost only at the tokamaks with divertor [4,5].

It is very important to demonstrate these favorable ability in a reactor grade tokamak and to extraporate a poloidal divertor to a reactor. In a reactor, only a shallow open divertor with a small burial chamber could be applied. JT-60 is a large tokamak with a simple poloidal divertor like that. The initial experiment was carried out from April to June in 1985 and stable 1.6 MA divertor discharge was obtained [6].

In this paper, radiation loss and global energy balance are discussed. Experiments are performed with ohmically heated hydrogen discharges: plasma current I_p of (0.5 ~ 1.6) MA, toroidal field B_T of (3 ~ 4) T, line-average electron density $\bar{n}_e$ of (0.5 ~ 4) $\times 10^{19}$ m^{-3}. Major and minor radii are 3.15 m and 0.83 m, respectively.

In the following section, experimental arrangements are described. Requirement for divertor effects are treated in section 3. Section 4 deals with the characteristics of radiation loss. Global energy balance is discussed in section 5. Impurity behavior is treated in section 6. In section 7, summary and conclusion are presented.

2. EXPERIMENTAL ARRANGEMENTS

Figure 1 shows the poloidal cross section of JT-60. It has a poloidal divertor on the outer equatorial plane. The first wall consists of toroidal limiters (Mo), liners (Inconel 625) and divertor

plates (Mo). Their surfaces are all coated with 20 μm titanium carbide.

Diagnostics related to our discussions are as follows;

1) filtered photo-diode (HAMAMATSU G1737) viewing H_α emission from divertor plasma (1ch): this is related to the intensity of particle flux to the divertor chamber.
2) calibrated 4-ch (main plasma) and 1-ch (divertor plasma) bolometers: they measure electromagnetic and neutral particle radiation. Radiation profile in main plasma is inferred by the 4-channel bolometer array. They are calibrated by the following technique [7]. As the bolometer is of thinister type (VECO 51K1C200), known electric power can be supplied through its lead wires. By using the resistance-temperature relation measured beforehand, heat capacity is obtained from the balance of this heating and cooling effect. The calibration accuracy is about 6 %.
3) thermo-couples mounted on the back of the divertor plates: they give time-integrated heat energy deposited in the divertor plates with the assumption of adiabatic temperature rise of the divertor plates.
4) Visible TV system: this shows plasma-limiter interaction by normally viewing main plasma.

TV image shows that main plasma is detached from the toroidal limiters with divertor operation. Therefore toroidal symmetry of radiation in main and divertor plasma, and heat deposition in divertor plates is expected. So we can estimate the total energy loss from the measured values in one poloidal cross section.

3. MINIMUM CLEARANCE FOR DIVERTOR ACTION

Particle and energy exhaust is expected as one of the divertor functions. This action to be effective, it is important to keep the sufficient width between the separatrix magnetic surface and wall. In JT-60, the width is limited by the toroidal limiters installed at 30° from the equatorial plane. This clearance is called δ_{30} (see Fig. 1). To investigate the critical value, δ_{30} was scanned from 4 to 2 cm during a discharge. δ_{30} is determined by magnetic analysis.

Figure 2(a) shows δ_{30}-dependance of H_α emission in divertor plasma (H_α^{div}) which is related to particle flux into the divertor chamber. Taking into account the accuracy of magnetic analysis, δ_{30} narrower than 2 ~ 3 cm leads H_α^{div} to significant decrease. This is because the particle

plates (Mo). Their surfaces are all coated with 20 μm titanium carbide.

Diagnostics related to our discussions are as follows;

1) filtered photo-diode (HAMAMATSU G1737) viewing H_α emission from divertor plasma (1ch): this is related to the intensity of particle flux to the divertor chamber.
2) calibrated 4-ch (main plasma) and 1-ch (divertor plasma) bolometers: they measure electromagnetic and neutral particle radiation. Radiation profile in main plasma is inferred by the 4-channel bolometer array. They are calibrated by the following technique [7]. As the bolometer is of thinister type (VECO 51K1C200), known electric power can be supplied through its lead wires. By using the resistance-temperature relation measured beforehand, heat capacity is obtained from the balance of this heating and cooling effect. The calibration accuracy is about 6 %.
3) thermo-couples mounted on the back of the divertor plates: they give time-integrated heat energy deposited in the divertor plates with the assumption of adiabatic temperature rise of the divertor plates.
4) Visible TV system: this shows plasma-limiter interaction by normally viewing main plasma.

TV image shows that main plasma is detached from the toroidal limiters with divertor operation. Therefore toroidal symmetry of radiation in main and divertor plasma, and heat deposition in divertor plates is expected. So we can estimate the total energy loss from the measured values in one poloidal cross section.

3. MINIMUM CLEARANCE FOR DIVERTOR ACTION

Particle and energy exhaust is expected as one of the divertor functions. This action to be effective, it is important to keep the sufficient width between the separatrix magnetic surface and wall. In JT-60, the width is limited by the toroidal limiters installed at 30° from the equatorial plane. This clearance is called δ_{30} (see Fig. 1). To investigate the critical value, δ_{30} was scanned from 4 to 2 cm during a discharge. δ_{30} is determined by magnetic analysis.

Figure 2(a) shows δ_{30}-dependance of H_α emission in divertor plasma (H_α^{div}) which is related to particle flux into the divertor chamber. Taking into account the accuracy of magnetic analysis, δ_{30} narrower than 2 ~ 3 cm leads H_α^{div} to significant decrease. This is because the particle

flow to the divertor chamber is blocked by 30°-limiters. So it is required to keep it wider than this value for sufficient particle exhaust. In Fig. 2(b), radiation in divertor plasma (P_R^{div}) also decreases significantly below δ_{30} of 2 ~ 3 cm. So δ_{30} wider than 2 ~ 3 cm is required for particle exhaustion and heat removal to be effective. Experimental results shown in the following were performed keeping δ_{30} above this critical value.

Figure 3 shows typical waveforms of plasma current and radiation loss in main plasma. In this figure, the upper line indicates P_R^{main} in the limiter discharge and the other line P_R^{main} in the divertor discharge ($\bar{n}_e$ is slightly higher in this case). In contrast to the limiter discharge, P_R^{main} settles down early to low level in the divertor discharge. This indicates that impurity influx to main plasma is suppressed to low level with divertor operation.

4. THE CHARACTERISTICS OF RADIATION LOSS

To estimate the total radiation power, relative signals of four bolometers viewing main plasma are compared with the calculated results for some axisymmetric model profiles shown in Fig. 4(d). In a limiter discharge, typical radiation profile at the beginning of the current flattop, when density is low about 1×10^{19} m^{-3}, is recognized to be parabolic (Fig. 4(a)) and radiated power is estimated to be 0.8 MW in the case of 1 MA discharge. At the end of the flattop, where energy balance is discussed in the following, bolometer signals lie in the region between calculated results for flat and periphery-peaked profiles (Fig. 4(b)). Radiation power at this time is halved to 0.4 MW. In a typical divertor discharge, radiation profile during the flattop shows the almost steady shape with poloidal asymmetry on the divertor side (Fig. 4 (c)). Radiation profile is taken to be flat (②) in calculating the total radiation power. It makes difference only by 13 % whether the profile is taken to be flat (②) or periphery-peaked profile (①). The error by neglecting the asymmetric component is about 20 %. Taking into account the accuracy of calibration (6 %), expected total error of P_R^{main} value is below 25 %.

Figure 5 shows radiation in main and divertor plasma (P_R^{main}, P_R^{div}) and the product of plasma current and the surface voltage ($I_P \times V_S$) as a function of plasma current. In limiter discharges (Fig. 5(a)),

flow to the divertor chamber is blocked by 30°-limiters. So it is required to keep it wider than this value for sufficient particle exhaust. In Fig. 2(b), radiation in divertor plasma (P_R^{div}) also decreases significantly below δ_{30} of 2 ~ 3 cm. So δ_{30} wider than 2 ~ 3 cm is required for particle exhaustion and heat removal to be effective. Experimental results shown in the following were performed keeping δ_{30} above this critical value.

Figure 3 shows typical waveforms of plasma current and radiation loss in main plasma. In this figure, the upper line indicates P_R^{main} in the limiter discharge and the other line P_R^{main} in the divertor discharge ($\bar{n}_e$ is slightly higher in this case). In contrast to the limiter discharge, P_R^{main} settles down early to low level in the divertor discharge. This indicates that impurity influx to main plasma is suppressed to low level with divertor operation.

4. THE CHARACTERISTICS OF RADIATION LOSS

To estimate the total radiation power, relative signals of four bolometers viewing main plasma are compared with the calculated results for some axisymmetric model profiles shown in Fig. 4(d). In a limiter discharge, typical radiation profile at the beginning of the current flattop, when density is low about 1×10^{19} m^{-3}, is recognized to be parabolic (Fig. 4(a)) and radiated power is estimated to be 0.8 MW in the case of 1 MA discharge. At the end of the flattop, where energy balance is discussed in the following, bolometer signals lie in the region between calculated results for flat and periphery-peaked profiles (Fig. 4(b)). Radiation power at this time is halved to 0.4 MW. In a typical divertor discharge, radiation profile during the flattop shows the almost steady shape with poloidal asymmetry on the divertor side (Fig. 4 (c)). Radiation profile is taken to be flat (②) in calculating the total radiation power. It makes difference only by 13 % whether the profile is taken to be flat (②) or periphery-peaked profile (①). The error by neglecting the asymmetric component is about 20 %. Taking into account the accuracy of calibration (6 %), expected total error of P_R^{main} value is below 25 %.

Figure 5 shows radiation in main and divertor plasma (P_R^{main}, P_R^{div}) and the product of plasma current and the surface voltage ($I_P \times V_S$) as a function of plasma current. In limiter discharges (Fig. 5(a)),

$P_R^{main}/I_P \times V_S$ tends to increase with I_P and it is about 60 % at 1.6 MA. In divertor discharges (Fig. 5(b)), P_R^{div} increases with I_P, attaining the value of 0.35 MW at 1.5 MA, and P_R^{main} tends to saturate with current-increase. In this figure, each $I_P \times V_S$ is an almost steady value and can be considered to be the ohmic input power. Therefore the ratio of P_R^{main} to the input power decreases with current-increase and attains 20 % at 1.5 MA.

In Fig. 6, $I_P \times V_S$, P_R^{main} and P_R^{div} are shown as a function of main plasma density in the case of divertor discharge. $I_P \times V_S$ and P_R^{main} increases slowly with $\bar{n}_e$ (Fig. 6(a), (b)).

P_R^{div} shows interesting feature (Fig. 6(c)). In low density regime, it increases with $\bar{n}_e$ and saturates at certain $\bar{n}_e$ value. At further high $\bar{n}_e$, it begins decreasing. The reason of this decrease is not clear at present.

5. GLOBAL ENERGY BALANCE

The diverted energy from the main plasma into the divertor chamber is dissipated by heat deposition onto the divertor plates as well as by radiation loss described above. Figure 7 shows global energy balance including the heat deposition in the plates. In this figure, each value is time-integrated energy over the current flattop period and their meanings are;

- Q_{in} : time-integrated value of $I_P \times V_S$ (almost equal to the ohmic input energy in this figure)
- Q_R^{main} : radiation energy in the main chamber
- Q_R^{div} : radiation energy in the divertor chamber
- Q_C^{div} : heat energy deposited in the divertor plates

The sum of Q_R^{main}, Q_R^{div} and Q_C^{div} almost balances with Q_{in} and 70 ~ 100 % of input energy is accounted. Therefore $Q_R^{div} + Q_C^{div}$, which reaches about 70 % of input energy, is diverted energy into the divertor chamber through the scrape-off layer. About a half of it is due to radiation loss. Such remote radiative cooling plays an important role from a viewpoint of heat load reduction of divertor plates.

$P_R^{main}/I_P \times V_S$ tends to increase with I_P and it is about 60 % at 1.6 MA. In divertor discharges (Fig. 5(b)), P_R^{div} increases with I_P, attaining the value of 0.35 MW at 1.5 MA, and P_R^{main} tends to saturate with current-increase. In this figure, each $I_P \times V_S$ is an almost steady value and can be considered to be the ohmic input power. Therefore the ratio of P_R^{main} to the input power decreases with current-increase and attains 20 % at 1.5 MA.

In Fig. 6, $I_P \times V_S$, P_R^{main} and P_R^{div} are shown as a function of main plasma density in the case of divertor discharge. $I_P \times V_S$ and P_R^{main} increases slowly with $\bar{n}_e$ (Fig. 6(a), (b)).

P_R^{div} shows interesting feature (Fig. 6(c)). In low density regime, it increases with $\bar{n}_e$ and saturates at certain $\bar{n}_e$ value. At further high $\bar{n}_e$, it begins decreasing. The reason of this decrease is not clear at present.

5. GLOBAL ENERGY BALANCE

The diverted energy from the main plasma into the divertor chamber is dissipated by heat deposition onto the divertor plates as well as by radiation loss described above. Figure 7 shows global energy balance including the heat deposition in the plates. In this figure, each value is time-integrated energy over the current flattop period and their meanings are;

- Q_{in} : time-integrated value of $I_P \times V_S$ (almost equal to the ohmic input energy in this figure)
- Q_R^{main} : radiation energy in the main chamber
- Q_R^{div} : radiation energy in the divertor chamber
- Q_C^{div} : heat energy deposited in the divertor plates

The sum of Q_R^{main}, Q_R^{div} and Q_C^{div} almost balances with Q_{in} and 70 ~ 100 % of input energy is accounted. Therefore $Q_R^{div} + Q_C^{div}$, which reaches about 70 % of input energy, is diverted energy into the divertor chamber through the scrape-off layer. About a half of it is due to radiation loss. Such remote radiative cooling plays an important role from a viewpoint of heat load reduction of divertor plates.

6. IMPURITY BEHAVIOR

Impurity behavior is investigated by the time dependence of radiation. Radiation profile is almost unchanged for a few second current flattop (Fig. 8) and no internal MHD oscillation is observed during this period [8]. This fact indicates that impurity accumulation around axis is not occurred even without internal MHD oscillation. Gross impurity confinement time is measured by switching of configuration from limiter toodivertor during current flattop. Figure 9 shows the time dependence of bolometer signal viewing the plasma center. Gross impurity confinement time is estimated from the decay time after the transition to divertor configuration and it is about 340 msec for the following plasma parameters and this value is in the same order as energy confinement time [9]; I_P = 0.5 MA, B_T = 3 T, $\bar{n}_e \geq 1 \times 10^{19}$ m^{-3}. Detail discussions need spectroscopic data.

7. SUMMARY AND CONCLUSION

Following divertor effects are obtained in the initial ohmic heating experiment of JT-60. When clearance δ_{30} is kept more than 2~3 cm. Radiation loss in main plasma is reduced to about 20 % of ohmic input power and this ratio tends to decrease with increase in plasma current. (In limiter discharges, $P_R^{main} / I_P \times V_S$ tends to increase with current and reaches to 60 % at 1.6 MA). Good heat and particle exhaust were performed. Almost 70 % of input energy is exhausted from the main chamber into the divertor chamber and about a half of it is due to radiation loss.

Impurity accumulation around the axis is not observed for a few sec without internal MHD activity and impurity confinement time is several hundred msec.

ACKNOWLDEGEMENTS

We thank all the members of the JT-60 Project who have long dedicated themselves to the construction of JT-60.

Our thanks are also due to the JT-60 operation team who conducted the first operation of JT-60 and contributed to implement the present series of experiments. We also thank Dr. S. Mori for his major role in initiating the JT-60 Project. We are grateful to Drs. K. Tomabechi,

6. IMPURITY BEHAVIOR

Impurity behavior is investigated by the time dependence of radiation. Radiation profile is almost unchanged for a few second current flattop (Fig. 8) and no internal MHD oscillation is observed during this period [8]. This fact indicates that impurity accumulation around axis is not occurred even without internal MHD oscillation. Gross impurity confinement time is measured by switching of configuration from limiter toodivertor during current flattop. Figure 9 shows the time dependence of bolometer signal viewing the plasma center. Gross impurity confinement time is estimated from the decay time after the transition to divertor configuration and it is about 340 msec for the following plasma parameters and this value is in the same order as energy confinement time [9]; I_P = 0.5 MA, B_T = 3 T, $\bar{n}_e \geq 1 \times 10^{19}$ m^{-3}. Detail discussions need spectroscopic data.

7. SUMMARY AND CONCLUSION

Following divertor effects are obtained in the initial ohmic heating experiment of JT-60. When clearance δ_{30} is kept more than 2$\sim$3 cm. Radiation loss in main plasma is reduced to about 20 % of ohmic input power and this ratio tends to decrease with increase in plasma current. (In limiter discharges, $P_R^{main} / I_P \times V_S$ tends to increase with current and reaches to 60 % at 1.6 MA). Good heat and particle exhaust were performed. Almost 70 % of input energy is exhausted from the main chamber into the divertor chamber and about a half of it is due to radiation loss.

Impurity accumulation around the axis is not observed for a few sec without internal MHD activity and impurity confinement time is several hundred msec.

ACKNOWLDEGEMENTS

We thank all the members of the JT-60 Project who have long dedicated themselves to the construction of JT-60.

Our thanks are also due to the JT-60 operation team who conducted the first operation of JT-60 and contributed to implement the present series of experiments. We also thank Dr. S. Mori for his major role in initiating the JT-60 Project. We are grateful to Drs. K. Tomabechi,

M. Yoshikawa, T. Iijima for their continued leaderships and supports. Drs. Y. Shimomura, S. Seki, M. Nagami, S. Konoshima and Experimental Group colleagues are gratefully ackowledged for their continuous discussions.

References

[1] DIVA GROUP. Nucl. Fusion 18 (1978) 1619.

[2] NAGAMI, M., FUJISAWA, N., IOKI, K., KITSUNEZAKI, A., KONOSHIMA, S., et al, in Plasma Physics and Controlled Nuclear Fusion Research (Proc. 8th Int. Conf. Brassels. 1980) Vol. 2, 367.

[3] KEILHACKER, M., ALBELT, D.B., BEHRINGER, KEHRISCH, R., ENGELHARDT, W., et al., ibid., Vol. 2, 351.

[4] WAGNER, F., et al, in Proc. 9th Int. Conf. on Plasma Physics and Controlled Nuclear Fusion Research, Baltimore, MD, 1982, Vol. 1 (IAEA, Vienna, 1982) p.43.

[5] KITSUNEZAKI, A., et al., in Plasma Physics and Controlled Nuclear Fusion Research (Proc. 10th Int. Conf. London, 1984) Vol. 1 (IAEA, Vienna, 1985) p.57.

[6] YOSHIKAWA, M., and JT-60 Team, in Controlled Fusion and Plasma Physics (Proc. 12th Europ. Conf. Budapest, 1985).

[7] Hsieh, C., GA Technologies, private communication, November 1980.

[8] JT-60 Team (presented by S. Tsuji)., in Controlled Fusion and Plasma Physics (Proc. 12th Europ. Conf. Budapest, 1985).

[9] M. Yoshikawa, Bull. Am. Phys. Soc. 30 (1985) 1362.

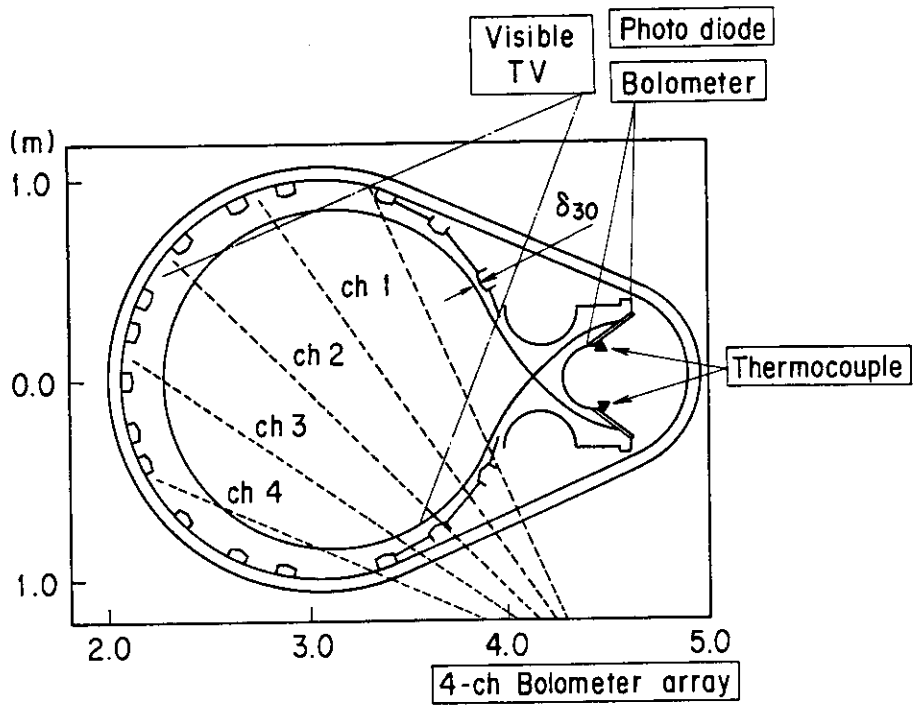

Fig. 1 Poloidal cross-sectional view of JT-60 with separatrix surface and arrangement of diagnostics relevant to energy balance study. Ch 1 ~ 4 indicates the chord number of bolometers. δ_{30} is the minimum clearance between toroidal limiters and the separatrix magnetic surface.

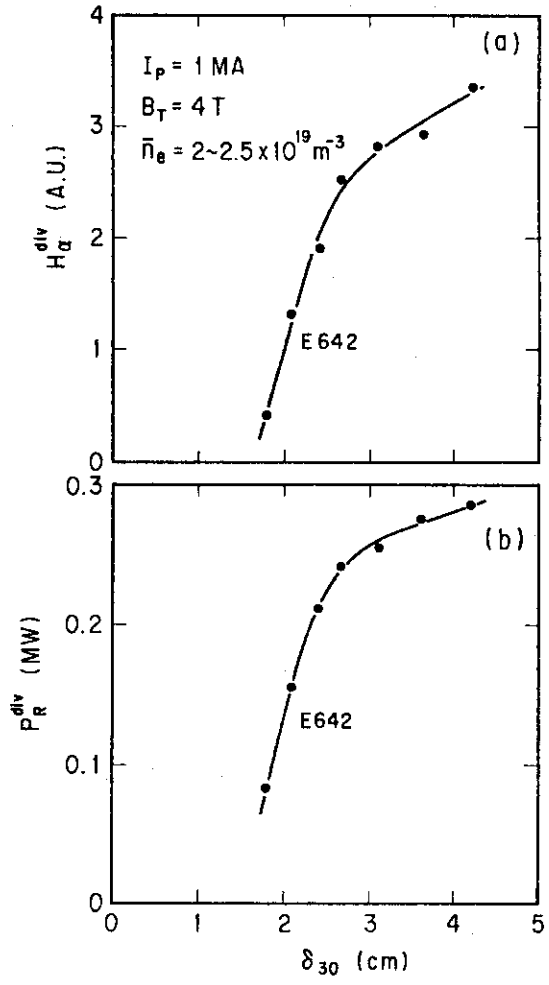

Fig. 2 (a) H_α and (b) bolometric signal in divertor plasma as a function of δ_{30}. 'E642' indicates the shot number.

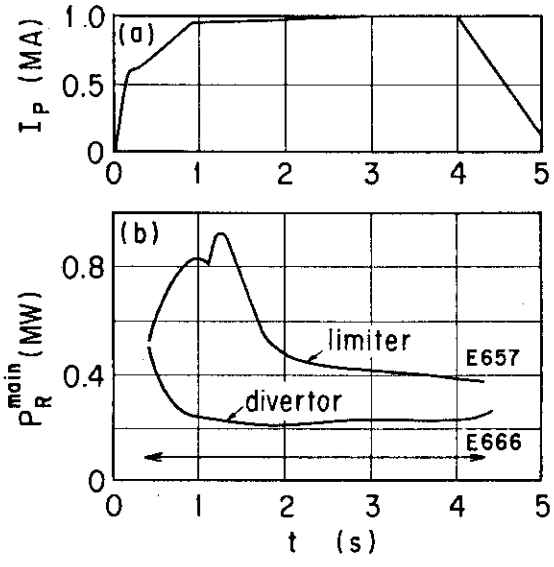

Fig. 3 (a) Typical wave forms of plasma current (I_P) and (b) radiation loss in main plasma (P_R^{main}) in the case of limiter and divertor discharges. In the latter case, divertor configuration is formed in the period indicated by an arrow and impurity influx is suppressed.

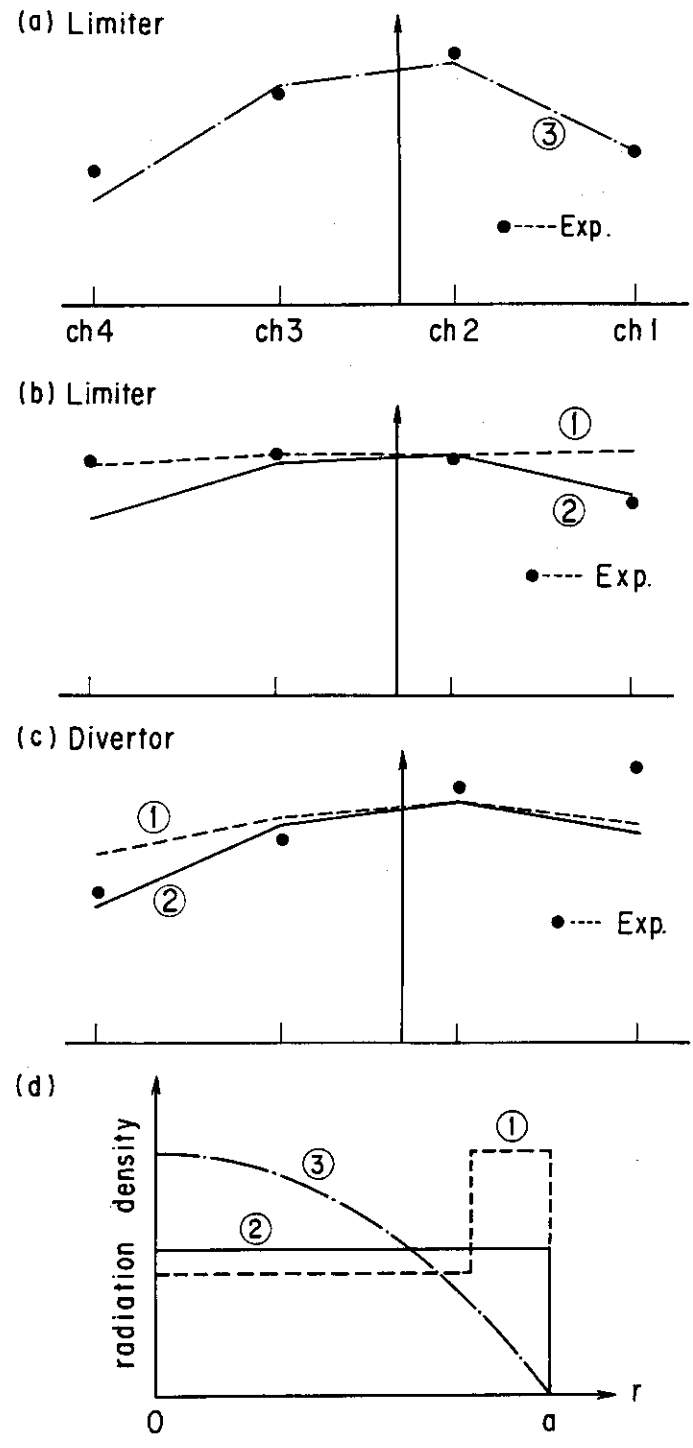

Fig. 4 Relative signals of bolometer array. Closed circles are experimental results and lines are calculated results for some axisymmetric profiles;

(a) limiter discharge at the beginning of the current flattop.

(b) limiter discharge at the end of the current flattop,

(c) divertor discharge at the end of the flattop,

(d) axisymmetric radiation profiles for calculation.

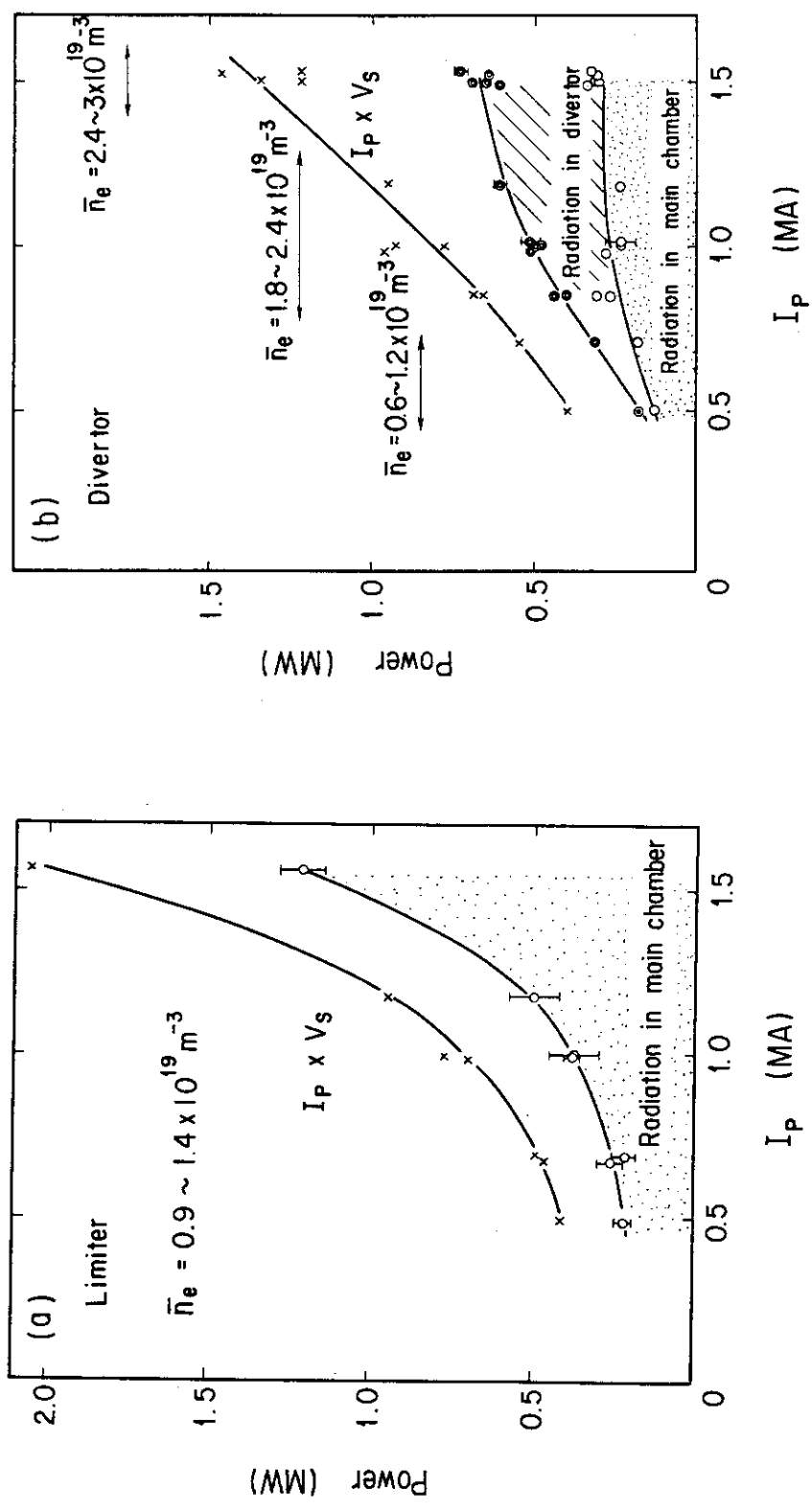

Fig. 5 Power balance of (a) limiter discharges, (b) divertor discharges. The product of I_P and Vs ($Ip \times V_s$), radiation power in main and divertor plasmas (R_R^{main}, P_R^{div}) as a function of Ip. In the divertor discharge, the ratio of P_R^{main} to ohmic input power decreases as current-increase.

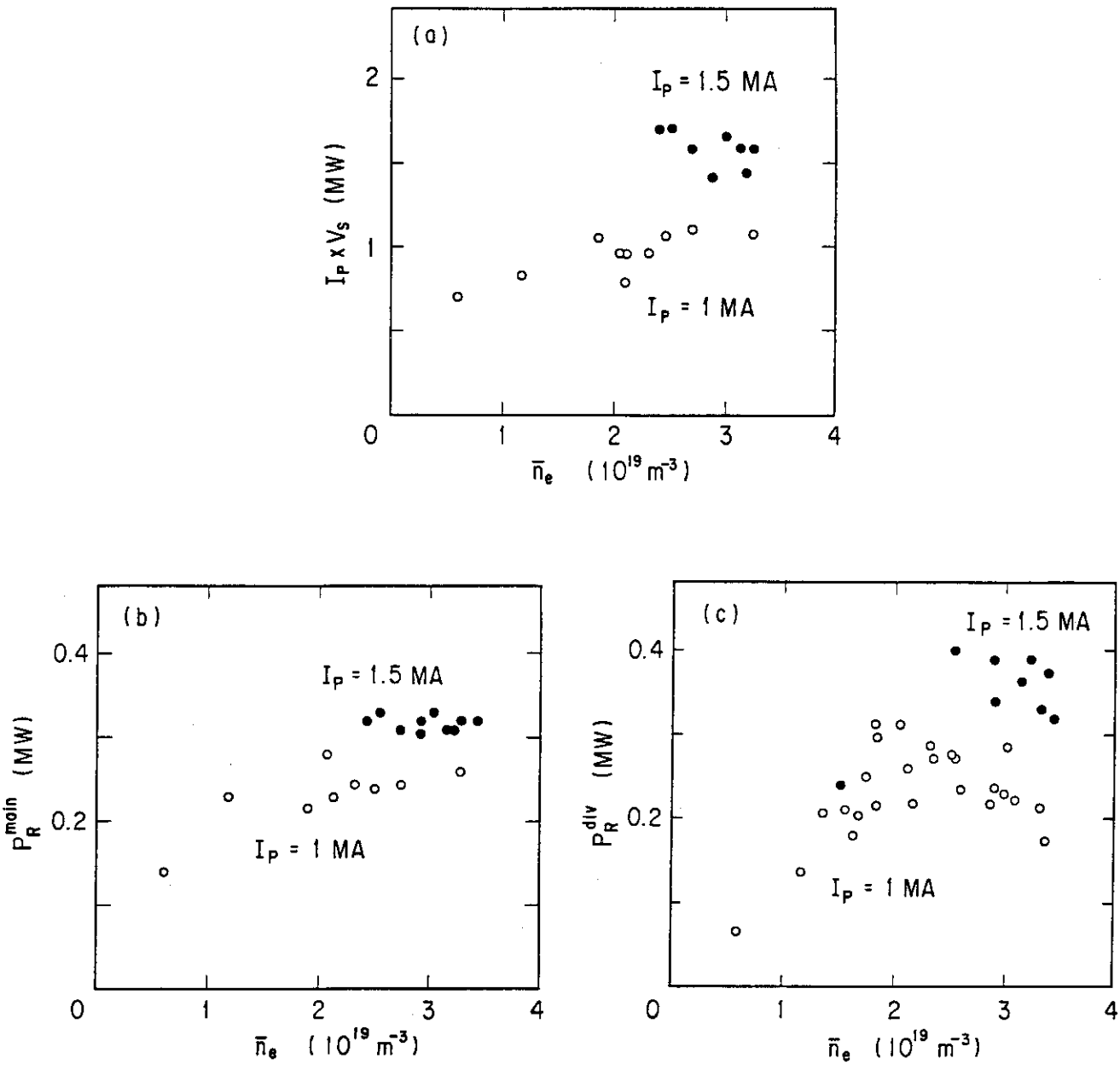

Fig. 6 (a) The product of Ip and the surface voltage V_s and radiation loss in (b) main (P_R^{main}) and (c) divertor (P_R^{div}) plasma as a function of main plasma density ($\bar{n}_e$). Open and closed circles shows the data of 1 MA and 1.5 MA, respectively. P_R^{main} and Ip × V_s show only a little change. P_R^{div} takes a maximum value at certain density.

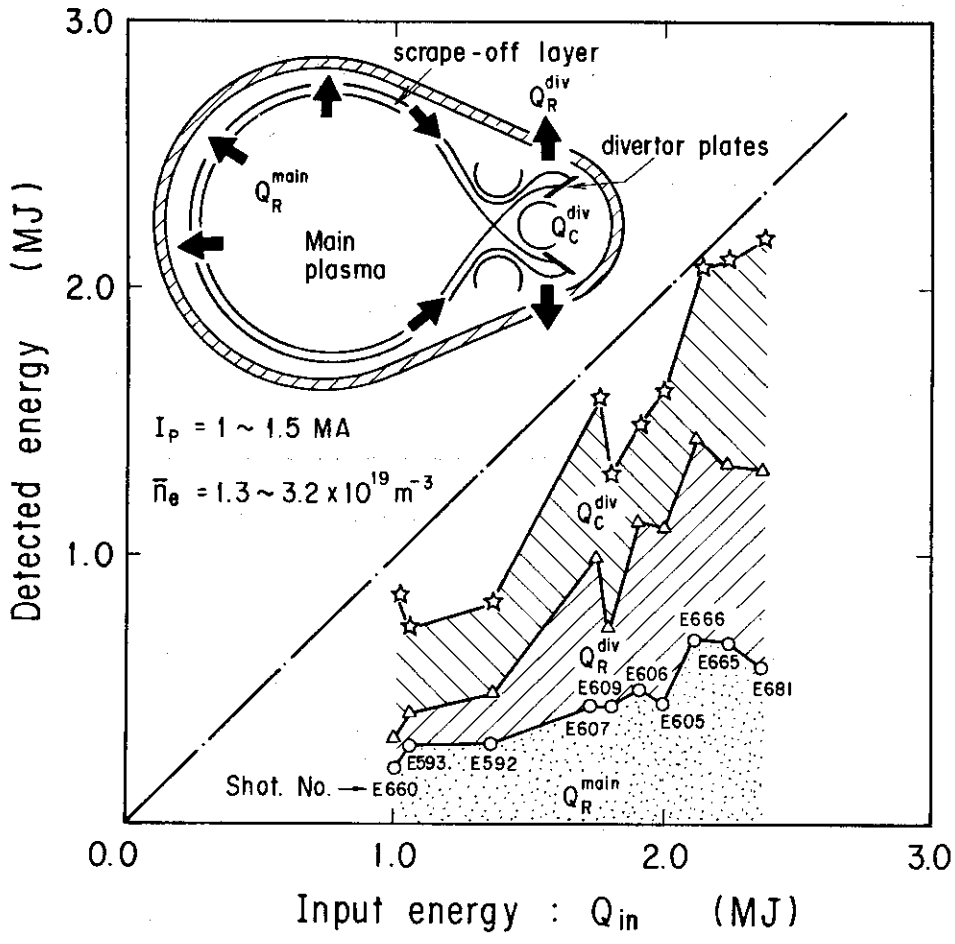

Fig. 7 Energy balance of diverted dischargs. Ohmic input energy (Q_{in}), radiation energies in main (Q_R^{main}) and divertor (Q_R^{div}) plasmas and heat deposition in divertor plates (Q_C^{div}). About 70 % of input energy are exhausted into divertor chamber and fair amount of them is dissipated by radiation loss.

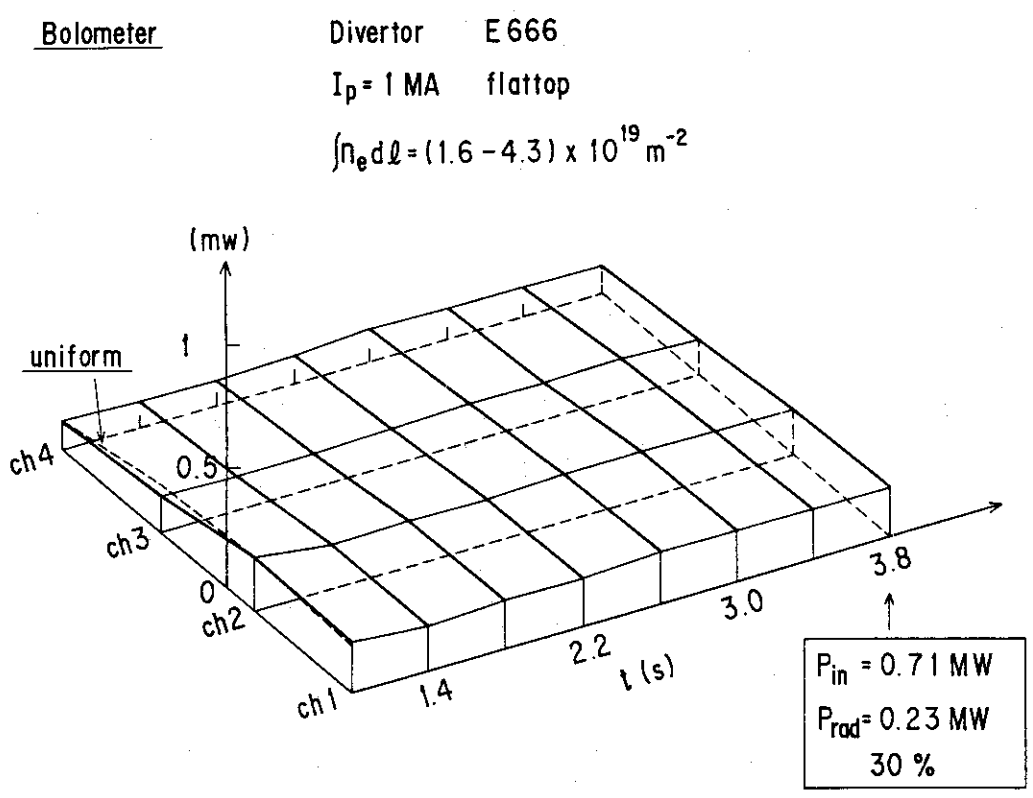

Fig. 8 Detected power of each bolometer during current flattop. Relative values between them is almost unchanged during this period.

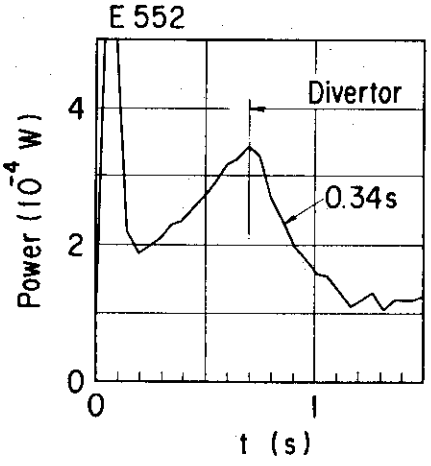

Fig. 9 Detected power of the center-viewing bolometer. Its decay time after transition to divertor configuration gives gross impurity confinement time.